Ab initio calculation of surface-resistivity induced by 3*d* adatoms on simple metals

M. I. Trioni,[1] H. Ishida,[2] and G. P. Brivio[1,3]
[1]*Istituto Nazionale per la Fisica della Materia - UdR Milano Bicocca, via Cozzi 53, 20125 Milano, Italy*
[2]*College of Humanities and Sciences, Nihon University, Sakura-josui, Tokyo 156, Japan*
[3]*Dipartimento di Scienza dei Materiali, Università di Milano ''Bicocca,'' via Cozzi 53, 20125 Milano, Italy*
(Received 9 June 2000; revised manuscript received 7 September 2000; published 30 January 2001)

We report on density-functional calculations of the surface resistivity ρ_s induced by isolated 3*d* adatoms on metal substrates. In the present work, we concentrate on the case of nonmagnetic adatoms on semi-infinite Al-like jellium, and the effects of magnetism and atomic relaxations are left as a subject for future work. For a fixed adatom-substrate distance z_a, the calculated ρ_s follows a characteristic bell-shaped curve as a function of the 3*d* valence as in the case of bulk impurities. For all the elements up to Fe, ρ_s is found to become even larger than the residual resistivity for the corresponding impurities in bulk jellium when the adatoms are located by ~ 1 bohr outside jellium. Also, for these elements, the calculated ρ_s as a function of z_a attains a maximum before decaying exponentially at larger z_a. Detailed analyses of the induced density of states (DOS) indicate that such a maximum is explained in terms of the behavior of the *p* component of the adatom-induced DOS at the Fermi level, which is found to be significantly enhanced due to charge redistributions when the atom is very close to the surface.

DOI: 10.1103/PhysRevB.63.075408 PACS number(s): 73.20.At, 73.20.Hb, 73.25.+i

I. INTRODUCTION

The study of dilute alloys is one of the oldest subjects in solid state-physics. Among other topics, resistivity due to impurity atoms has been studied for a long time. By the 1930s, it was known that magnetic impurities such as Fe and Mn give rise to a minimum in the resistivity of a host metal as a function of temperature; the origin of this was not clarified until the pioneering work of Kondo.[1] The theoretical study of the electronic structure of impurity atoms within the one-electron approximation was initiated by Friedel.[2] For a single-impurity atom in a uniform electron gas (jellium), the carrier scattering by the impurity potential is characterized by $\delta_l(\epsilon)$, the phase shift of a partial wave with angular momentum *l* at energy ϵ. The residual resistivity, i.e., the resistivity at zero temperature via impurity scattering, is given by

$$\rho_b = \frac{4\pi\hbar}{V n_e e^2 k_F} \sum_{l \geqslant 0} (l+1) \sin^2[\delta_{l+1}(\epsilon_F) - \delta_l(\epsilon_F)], \quad (1)$$

where *V* is the volume per impurity atom, ϵ_F is Fermi level, $k_F = \hbar^{-1}\sqrt{2m\epsilon_F}$, and n_e denotes the electron density. Assuming that $\delta_{l=2}(\epsilon_F)$ dominates for 3*d* impurity atoms in an *sp* host metal, and that these atoms have no magnetic moments, and also combining (1) and the Friedel sum rule, one obtains $\rho_b = (4\pi\hbar/V n_e e^2 k_F) 5 \sin^2(\pi\tilde{Z}/10)$. This implies that ρ_b may follow a bell-shaped curve as a function of the 3*d* valence occupancy $\tilde{Z}$, with a maximum located at around Cr and Mn. This behavior was experimentally confirmed for dilute Al alloys.[3] On the theory side, the resistivity due to substitutional 3*d* atoms in jellium with an electron density corresponding to Al was calculated by Mrosan and Lehman[4] and Niemenen and Puska.[5] Following more realistic ground-state electronic calculations of impurities in transition metals with a lattice structure, performed by using a Korringa-Kohn-Rostoker Green-function method,[6,7] the resistivity curve for 4*d* impurities in Cu was computed by solving the linearized Boltzmann equation. It exhibits a maximum at Nb with a nearly half-filled 4*d* shell, as explained above.[8]

The resistivity of a thin metal film is very sensitive to surface conditions when the temperature is as low as 10 K.[9] Defects such as steps and adsorbates scatter conduction electrons impinging on the surface diffusively, leading to an increase in resistivity. Although the theory of the surface resistivity dates back to the semiclassical model of Fuchs,[10] (also see Ref. 11), it was only recently that a microscopic expression of the surface resistivity at the same level as Eq. (1) was derived for the case of semi-infinite metals.[12] As will be discussed in Sec. II, the only input for this formula is the wave function (or Green's function) of electrons at ϵ_F appropriate for the semi-infinite geometry. So far only a few quantum-mechanical calculations of the surface resistivity were reported.[13–15]

The aim of the present paper is to investigate the residual resistivity induced by 3*d* atoms adsorbed on simple metal surfaces. In particular we will focus on elucidating features that are absent in the case of bulk impurities. From a theoretical viewpoint, the impurity atom on the surface has an additional degree of freedom: The induced resistivity ρ_s can be plotted on a two-dimensional plane as a function of the atomic number *Z*, and z_a, the adatom position relative to the substrate surface. We explore the dependence of ρ_s on both quantities by performing an extensive density-functional calculation. We adopt semi-infinite jellium[16] to simulate an Al-like substrate, and the semi-infinite problem is handled with the use of the embedding method of Inglesfield.[17] Although some of the 3*d* adatoms may have magnetic moments on Al, we will concentrate on the case of nonmagnetic impurity atoms in the present paper, and the effects of the magnetic moment on the residual resistivity will be left as a subject for future developments. Also, it should be noted that the substrate relaxations, observed and calculated in the ultrathin film growth of transition-metal atoms[18,19] cannot be taken

into account by the jellium substrate. For example, in this area, it was recently suggested that relaxation may modify electronic properties such as magnetic moments of $3d$ atom overlayers.[20] Instead, in the present work, we will shed light on general features of the induced resistivity that are insensitive to the detailed substrate atomic and local electronic structures, aiming at studying the effects of a single adatom on a semi-infinite solid. This may be justified, since, to our knowledge, there has been no theoretical work on the resistivity induced by transition-metal adatoms. We also observe that a more realistic calculation taking into account the substrate lattice structure remains very difficult.

At first glance, it may appear that ρ_s preserves its bell-shaped dependence along the Z axis, and decreases monotonically with increasing z_a, as does the overlap between the metal and $3d$ wave functions. However, as z_a increases, the $3d$ resonance becomes sharper and its center shifts gradually toward the Fermi energy. Consequently the adatom local density of states (DOS) at ϵ_F is enhanced. Furthermore, because of chemical interactions with substrate states, charge redistributions take place among the delocalized s and p states and the $3d$ shell. From our calculations it has turned out that these competing effects give rise to a nontrivial variation of ρ_s as a function of z_a.

The plan of the present paper is as follows. In Sec. II, we describe the method for computing the ground-state electronic structure and the induced resistivity of a single adatom on a semi-infinite jellium surface using the embedding Green-function approach for the isolated adsorbate.[21,22] Section III constitutes the main part of the present paper, and contains results and discussion of the numerical calculations. Section IV is devoted to conclusions. Unless otherwise stated, we use Hartree atomic units throughout this paper.

II. THEORY

We calculate the electronic structure of a single isolated adatom on a semi-infinite jellium surface[23] within the local-density approximation in density-functional theory (LDA-DFT).[24] We choose the z axis as the surface normal pointing toward the vacuum. The position of the adatom is $(0,0,z_a)$ and the positive background charge of jellium occupies the half-space $z \leqslant 0$. As the potential perturbation due to the adatom is spatially localized, we treat only a spherical region with radius R_s surrounding the adatom and containing a portion of jellium explicitly in the self-consistent procedure, whereas the effects of the rest of the jellium surface are taken into consideration via a complex embedding potential acting on the sphere surface. The Green function in the embedding sphere can be expanded as

$$G(\mathbf{r},\mathbf{r}',\epsilon)=\sum_{L,L'} G(L,r;L',r';\epsilon)Y_L(\Omega)Y^*_{L'}(\Omega'), \quad (2)$$

$$G(L,r,L',r',\epsilon)=\sum_{n,n'} G(L,n;L',n';\epsilon)\phi_{ln}(r)\phi_{l'n'}(r'), \quad (3)$$

where $L=(l,m)$. Inside the muffin-tin sphere with radius R_{MT}, the radial basis function $\phi_{ln}(r)$ is a linearized muffin-tin orbital, while $\phi_{ln}(r)=j_l(k_n r)$ for $R_{MT} \leqslant r \leqslant R_s$, where $k_n=\pi n/\tilde{a}$ ($n \geqslant 1$ and $\tilde{a} \geqslant R_s$).[25] More details of the ground-state calculation are described in Refs. 21 and 22.

We calculate the surface resistivity induced by a single atom adsorbed on semi-infinite jellium. First it should be noted that the clean jellium substrate has no resistivity, since conduction electrons impinging onto a perfectly flat surface are specularly reflected. On the other hand, in the presence of the adatom, the electrons are partly scattered in off-specular directions. The surface resistivity associated with a current density in the x direction is given by[12,13]

$$\rho_s=\frac{2\pi\hbar}{Vn_e^2e^2}\sum_{i,j}\delta(\epsilon_i-\epsilon_F)\delta(\epsilon_j-\epsilon_F)\left\langle\psi_i\left|\frac{\partial V_{\rm eff}}{\partial x}\right|\psi_j\right\rangle \times\left\langle\psi_j\left|\frac{\partial V_{\rm eff}}{\partial x}\right|\psi_i\right\rangle, \quad (4)$$

where $V_{\rm eff}$ denotes the one-electron effective potential in density-functional theory, and ψ_i is an electron wave function appropriate for the semi-infinite geometry. By using the Green function, Eq. (4) can be read as

$$\rho_s=\frac{2\hbar}{V\pi n_e^2e^2}\int d\mathbf{r}\,d\mathbf{r}'\,{\rm Im}\,G(\mathbf{r},\mathbf{r}',\epsilon_F)\frac{\partial V_{\rm eff}}{\partial x'} \times{\rm Im}\,G(\mathbf{r}',\mathbf{r},\epsilon_F)\frac{\partial V_{\rm eff}}{\partial x}. \quad (5)$$

As already mentioned, we consider a model substrate represented by jellium, for which we can explicitly calculate the induced resistivity using the Green function in the embedding region alone. In fact the x derivative of the potential, $\partial_x V_{\rm eff}$, is identically zero far from the adsorbate (outside the embedding region) (i) due to the assumption that metal electrons screen the impurity potential perfectly and (ii) due to the lack of lattice periodicity in the potential along any direction parallel to the surface [i.e., $V_{\rm eff}(\mathbf{r})=V(z)$].

To be more concrete, we make use of the cylindrical symmetry of the system about the z axis. The effective potential in the embedding sphere is expanded as[21,22]

$$V_{\rm eff}(\mathbf{r})=\sum_l V(l,r)Y_{l0}(\Omega). \quad (6)$$

Also, $G(L,n;L',n';\epsilon)$ in Eq. (3) is diagonal with respect to indices m and m'. Substituting Eqs. (2) and (6) into Eq. (5) yields

$$\rho_s=\frac{2\hbar}{V\pi n_e^2e^2}\sum_m\sum_{l_1\sim l_4}\sum_{n_1\sim n_4} \times{\rm Im}\,G(l_1,m,n_1;l_2,m,n_2)v_x(l_2,m,n_2;l_3,m\pm1,n_3) \times{\rm Im}\,G(l_3,m\pm1,n_3;l_4,m\pm1,n_4) \times v_x(l_4,m\pm1,n_4;l_1,m,n_1). \quad (7)$$

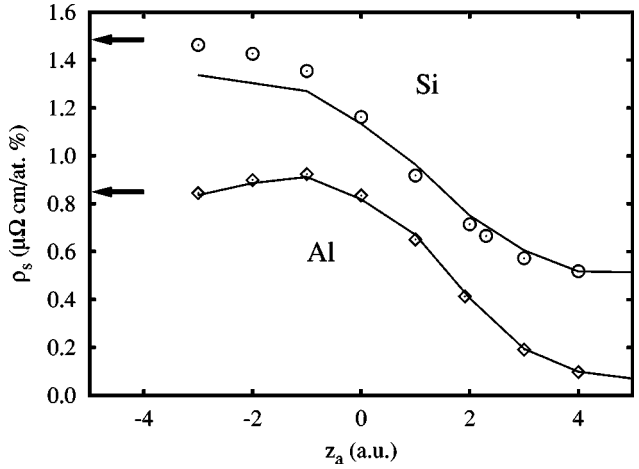

FIG. 1. Resistivity induced by a Si or Al adatom on Al-like jellium as a function of the adatom-surface distance z_a (solid lines). The results from Ref. 13 are also shown as diamonds and circles. The arrows on the left refer to the resistivity for an interstitial atomic impurity in Al-bulk jellium.

In the above, we omitted the energy suffix of the Green function, and the matrix element of $\partial_x V_{\rm eff}$ is defined by

$$
\begin{aligned}
&v_x(l_1,m,n_1;l_2,m\pm1,n_2)\\
&\quad=\mp\frac{1}{2}\sum_{l\geqslant 0}\sqrt{\frac{(l+1)(l+2)}{(2l+1)(2l+3)}}\\
&\qquad\times g(l_1,m;l+1,\mp1;l_2,m\pm1)v_l^+(l_1n_1,l_2n_2)\\
&\qquad\mp\frac{1}{2}\sum_{l\geqslant 2}\sqrt{\frac{l(l-1)}{(2l-1)(2l+1)}}\\
&\qquad\times g(l_1,m;l-1,\mp1;l_2,m\pm1)v_l^-(l_1n_1,l_2n_2),
\end{aligned}
\tag{8}
$$

where $g(L_1;L_2;L_3)=\int d\Omega Y^*_{L_1}Y_{L_2}Y_{L_3}$ is the Gaunt coefficient, and

$$
\begin{aligned}
v_l^+(l_1n_1,l_2n_2)&=\int_0^{R_s}r^2dr\,\phi_{l_1n_1}(r)\phi_{l_2n_2}(r)\\
&\quad\times\left(\frac{d}{dr}-\frac{l}{r}\right)V(l,r),
\end{aligned}
\tag{9}
$$

$$
\begin{aligned}
v_l^-(l_1n_1,l_2n_2)&=\int_0^{R_s}r^2dr\,\phi_{l_1n_1}(r)\phi_{l_2n_2}(r)\\
&\quad\times\left(\frac{d}{dr}+\frac{l+1}{r}\right)V(l,r).
\end{aligned}
\tag{10}
$$

III. RESULTS

First we consider Al and Si adatoms on an Al-like jellium surface, by varying the atom-jellium edge distance z_a ($z_a>0$ is toward vacuum). In Fig. 1 we show the induced resistivity ρ_s, where the arrows on the left refer to the resistivity for an ''interstitial'' atomic impurity in bulk jellium.[26] That is, the impurity nucleus is simply put into the bulk without removing the positive background charge of jellium surrounding it. Because the jellium substrate is unrelaxed, such a bulk result has just to be read as the asymptotic value of our resistivity calculation inside the metal. For comparison, we also present the calculated ρ_s for the same systems in Ref. 13 (circles and diamonds), where the surface resistivity was obtained by using the same equation [Eq. (5)]. However, in Ref. 13 the Green function was computed with a very different numerical method based on the Dyson equation, norm-conserving pseudopotentials, and a plane-wave-like basis set. In spite of this, the agreement between the two sets of results is very good, which may add credibility to both approaches. The interested reader is referred to Ref. 13 for a more detailed discussion about these results. Here we only recall that the induced resistivity for such atoms is less than 1.5 $\mu\Omega$ cm/at. %, and it decreases smoothly by increasing the atom-surface distance.

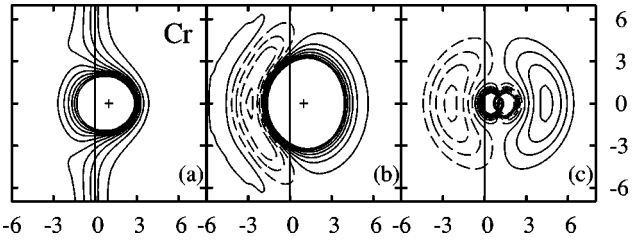

FIG. 2. Charge-density maps of a single Cr atom on Al-like jellium on a vertical cut plane containing the adatom at $z_a=1$ a.u. (a) Total charge density. (b) Local density of states at the Fermi level, $\sigma(\mathbf{r},\epsilon_F)$. (c) The dipolar part of $\sigma(\mathbf{r},\epsilon_F)$. Solid and dashed lines correspond to positive and negative values of the charge, respectively.

Now we consider $3d$ adatoms on the same Al-like jellium surface. Useful information on bonding may be obtained from the charge contours.[27] Thus in Fig. 2(a) we plot the total charge density on a vertical cut plane containing the adatom for Cr at $z_a=1$. This suggests that Cr may form a covalent metallic bond. Because the surface resistivity is determined by the one-electron states at the Fermi level, in Fig. 2(b) we show the contour map of the induced local density of states (DOS) at ϵ_F, $\sigma(\mathbf{r},\epsilon_F)$, which is defined by

$$
\sigma(\mathbf{r},\epsilon)=\frac{2}{\pi}\,\mathrm{Im}[G(\mathbf{r},\mathbf{r},\epsilon+i\delta)-G_0(\mathbf{r},\mathbf{r},\epsilon+i\delta)],
\tag{11}
$$

where G_0 denotes the Green function of the clean substrate, and $i\delta$ is a small imaginary energy. The appearance of a charge depletion area in the interface region in this map indicates that the charge density deviates strongly from a spherical distribution due to the adatom-substrate interaction. To demonstrate this, in Fig. 2(c) we also plot the dipole part (the $l=1$ component) of $\sigma(\mathbf{r},\epsilon_F)$. The main contribution to such a dipolar charge density can be attributed to the mixing of the p and d orbital components in the wave functions at ϵ_F. This point will be reconsidered below.

In Fig. 3 we present the induced resistivity of $3d$ adatoms at $z_a=1$ and 2 a.u. together with that of $3d$ interstitial im-

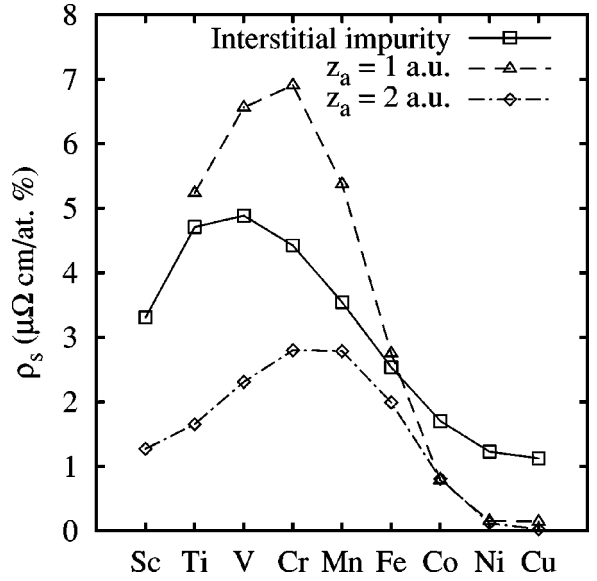

FIG. 3. Resistivity induced by $3d$ atoms on Al at adatom-surface distances $z_a=1$ a.u. (dashed line) and $z_a=2$ a.u. (dot–dashed line), and by interstitial (solid line) impurities in the Al bulk.

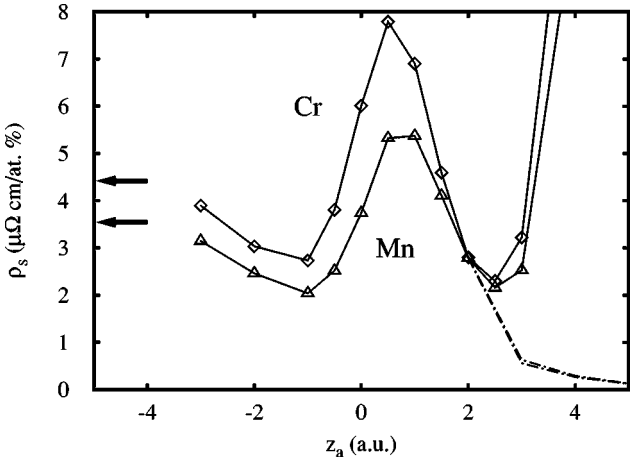

FIG. 4. Resistivity induced by a Cr or Mn adatom on Al as a function of the adatom-surface distance z_a. The arrows on the left refer to the resistivity for an interstitial atomic impurity in the Al bulk. LDA-DFT results are shown by solid lines, and EM results by dot-dashed lines.

purities. As stated above, such a bulk result only serves as the asymptotic value of our calculation at $z_a=-\infty$.[28] First of all we note that the bell shape of the induced-resistivity curve[5] is also reproduced for the adatoms. But, as compared with the results for interstitial impurities in bulk jellium (solid line), the maxima of the two curves are displaced toward the right. This can be explained using the simple equation discussed in the Sec. I, $\rho \propto \sin^2(\pi \tilde{Z}/10)$, where $\tilde{Z}$ is the calculated d orbital occupancy. In fact $\tilde{Z}$ is influenced by the Pauli repulsion between the s electrons of the metal and of the adatom, which determines a charge transfer between the atomic $4s$ and $3d$ levels. In particular, closer to the jellium edge is the atom, larger is the Pauli repulsion because of the large overlap of the s components of the metal and adatom wave functions, which then leads to a higher occupancy of the $3d$ level. Of course this effect attains its maximum for an interstitial impurity. That is, the $3d$ occupation for Cr and Mn increases by more than one electron as z_a changes from $z_a=+\infty$ (vacuum) to $-\infty$ (interstitial).

In Fig. 3, a feature which is absent in the induced resistivity for Si and Al manifests itself. For all the elements up to Fe, ρ_s for $z_a=1$ a.u. is larger than that of the corresponding impurities in the bulk.[28] This contrasts with what one may expect, i.e., that the perturbation induced by an atom on the surface would be smaller than that induced by a bulk impurity. Moreover, this remarkable behavior is not found for Co, Ni, and Cu. At $z_a=2$ a.u., the decay of the atom-surface perturbation dominates the above effect, and a progressive reduction of ρ_s is observed. Thus these results indicate the presence of a maximum in the induced resistivity as a function of the adatom-surface distance, except for these three elements. To confirm this behavior, in Fig. 4 we plot ρ_s as a function of z_a for Cr and Mn, and observe a different behavior from that of Si and Al. In fact, the calculated ρ_s (diamonds and triangles) starts from the asymptotic interstitial impurity values, reaches a maximum at $z_a \sim 0.8$ a.u., and then it decreases up to $z_a \sim 2.5$ a.u., and finally it starts rising again, tending to a divergent behavior. In the following, we shall discuss the origin of these unexpected features of ρ_s in detail.

First we clarify why a maximum appears in the resistivity curve. For this purpose, the analysis of the DOS may be useful. Figure 5 displays the total induced DOS in the embedding sphere at $z_a=1$ a.u. defined by $\sigma(\epsilon) = \int_{R_s} d\mathbf{r}\, \sigma(\mathbf{r},\epsilon)$. In Fig. 5 we observe that the $3d$ resonances are more sharply peaked than those of the same impurities in Al bulk (see Ref. 5). A detailed analysis of such a DOS shows that the degeneracy in the m quantum number, related to the z component of the angular momentum, is lifted. For example each m component (dashed lines) is plotted for the Cu adatom. Owing to this degeneracy resolution the $3d$ reso-

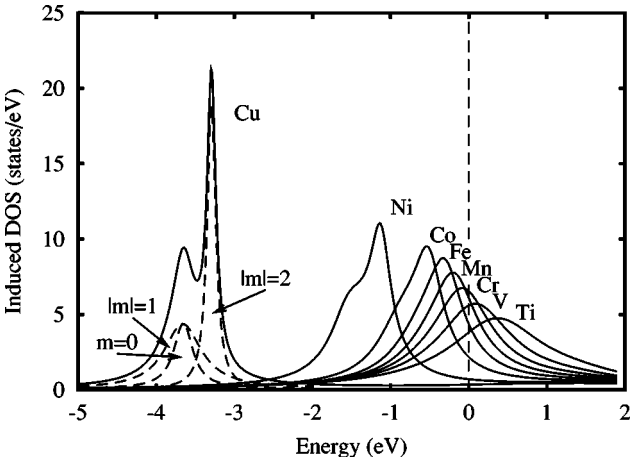

FIG. 5. Induced DOS of $3d$ atoms at an atom-surface distance $z_a=1$ a.u. on Al. The reference energy level is at the Fermi level. The $3d$ resonance of Cu is decomposed into its m components: $m=0$, $|m|=1$, and $|m|=2$.

nance is nonsymmetric around its maximum. The following simple expression, derived by Persson[29] from a Anderson-Grimley-Newns-type model Hamiltonian, helps one to understand the relationship between induced resistivity and the local DOS:

$$\rho_s = \frac{2m\epsilon_F}{V\hbar n_e^2 e^2}\langle \sin^2\theta\rangle \Gamma \sigma_a(\epsilon_F). \tag{12}$$

In Eq. (12), Γ is the width of the adsorbate resonance, $\sigma_a(\epsilon)$ is the DOS projected onto the adatom orbital, and the average $\langle \sin^2\theta\rangle$ defined in Ref. 29 is a weak function of z_a. The above equation indicates that ρ_s is determined by the energy position and width of the adatom resonance. Thus when the $3d$ resonance is strong and centered at about the Fermi energy, the induced resistivity may be enhanced. And this explains why the calculated ρ_s at $z_a=1$ a.u. for several $3d$ elements exceeds the resistivity for the corresponding bulk impurity. On the other hand, it has turned out that the maximum in the induced resistivity does not necessarily occur at that position of z_a where the induced DOS at ϵ_F is largest.

To illustrate this point, we examine the resistivity equation (5) more carefully. First we note that the higher potential components with $l \geqslant 1$ in Eq. (6) have nonvanishing values only when the adatom is near the jellium surface. Hence these potential components may give a maximum in the resistivity curve. But we have found that they contribute to only 10–20 % of the total resistivity, and that the z_a dependence of ρ_s in Fig. 4 can be well reproduced if just the spherical part of the potential $V(l=0,r)Y_{00}$ is considered. The above statement also holds even when $V_{\rm eff}$ in Eq. (5) is fixed at its asymptotic value at $z_a=-\infty$ for all the z_a values. So the maximum in the ρ_s curve originates from the imaginary part of the Green function in Eq. (5), and not from the potential derivative, and this property can be easily recast in terms of the properties of the induced DOS, $\sigma(\epsilon)$. Recall that the x derivative of the spherical potential changes angular momentum only by ± 1. Our calculation shows that the main contribution to the matrix elements in Eq. (7) arises from the cross terms of the p and d states. In Fig. 6, we plot the contribution of the p component of the wave functions at Fermi level to the induced DOS, $\sigma_p(\epsilon_F)$, and that for the d orbitals, $\sigma_d(\epsilon_F)$, as functions of z_a. It is seen that the former displays a maximum at $z_a \sim 0$. This, in turn, leads to an enhancement of the p-d cross terms in the matrix elements in Eq. (7) determining a maximum in the calculated ρ_s. In Fig. 6 we also show the product $\sigma_p(\epsilon_F)\sigma_d(\epsilon_F)$, whose curve as a function of z_a remarkably well reproduces the characteristic features of the resistivity curve in Fig. 4. As stated above, these p and d components are also strongly hybridized [see Fig. 2(c)]. Because the enhancement of the p component of the induced DOS near the surface may be a general feature for any $3d$ atom bonded to a metallic surface, a maximum in ρ_s, as a function of z_a, may appear for many combinations of adatoms and real metal substrates. For example, for the present Al-like jellium substrate, the maximum appears for all $3d$ elements up to Fe, and we have verified that the z_a coordinate corresponding to the maximum shifts toward the vacuum with increasing atomic number.

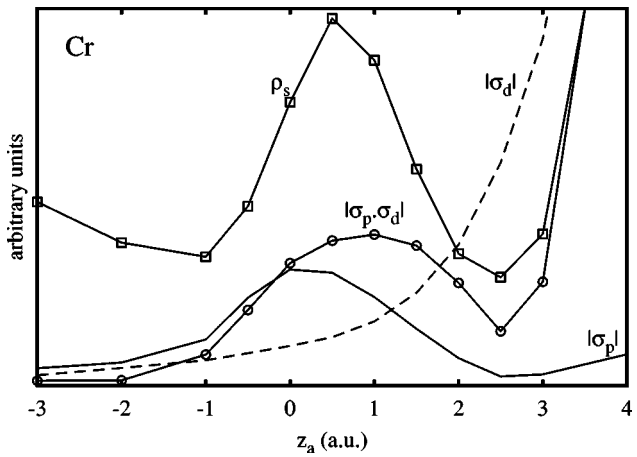

FIG. 6. Angular-momentum decomposition of the induced DOS of Cr at the Fermi level as a function of z_a for the p (solid line) and d (dashed line) components. Also plotted are their product $|\sigma_p(\epsilon_F)\cdot\sigma_d(\epsilon_F)|$ (circles) and the calculated resistivity of Cr (squares). The latter two curves are scaled so that they fit in the same graph.

Here it may be worth commenting on the effects of magnetism to the resistivity. As stated in Sec. I, some elements in the middle of the $3d$ series may have a magnetic moment on Al. For a magnetic adatom, ρ_s at zero temperature is obtained simply by evaluating Eq. (5) for both the majority- and minority-spin populations, and taking their average [note that Eq. (5) includes a factor 2 for spin]. In this case the induced DOS displays two peaks due to the majority- and minority-spin populations. Consequently the total induced DOS, summed over the spin, at the Fermi level is expected to show a double-peaked structure as a function of the atomic number Z, differently from the nonmagnetic case where there is only one maximum (see Fig. 5). This may lead to a decrease in surface resistivity for the atoms in the middle of the $3d$ series, as observed in the case of bulk magnetic impurities.[30] If so, the maximum in the resistivity curve that we found for Cr and Mn may be modified in a significant way. Because of these magnetic effects and also, since the equilibrium position of the adatom may not be in the range of z_a where ρ_s is enhanced, at present it is not clear whether the maximum in the resistivity can be observed experimentally. A realistic spin-dependent total-energy calculation that takes account of the substrate atomic structure is necessary in this respect.

Now we discuss the apparent divergent behavior of ρ_s at larger z_a ($z_a > 2$ a.u.). This behavior is certainly unphysical, since in this range of weaker atom-metal coupling one would expect ρ_s to decay exponentially as does the overlap of the adatom and substrate electron wave functions. In Fig. 7 we show the induced DOS for the Cr adatom at three different positions: $z_a=-1$, 1, and 3 a.u. When the atomic nucleus is close to the surface, but still inside the positive charge background of jellium, we observe that the $3d$ resonance is located at lower energies, essentially following the electrostatic potential of the clean surface.[23] On the other hand, the $3d$ resonance becomes sharply peaked around the Fermi energy for atom-surface distances $z_a \geqslant 3$ a.u. To elaborate on this

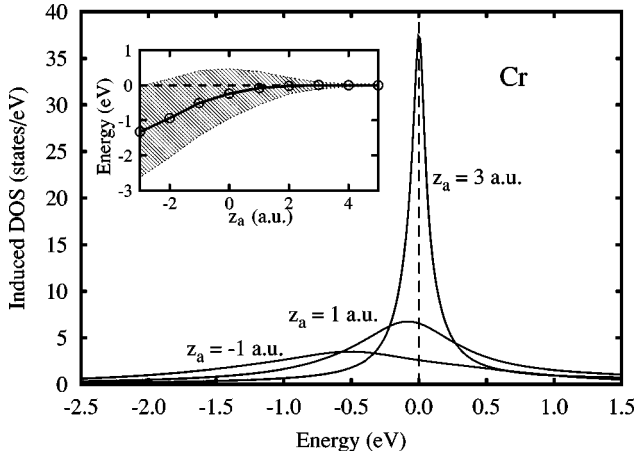

FIG. 7. Induced DOS of a Cr atom on Al at distances $z_a=-1$, 1, and 3 a.u. Inset: width (shaded area) and position (circles) of the $3d$ resonance of Cr as a function of z_a.

point further, we plot the width and the position of the Cr $3d$ resonance by increasing z_a in the inset of Fig. 7. Here one can clearly see that the LDA pins the almost δ-function-like atomic valence level at ϵ_F, and consequently the resistivity calculated with Eq. (5) tends to diverge, as does the imaginary part of the Green function. Such a behavior of the induced DOS occurs in any LDA-DFT approach like ours, where jellium and an atom with a partially occupied valence shell are described as if they kept interacting at any distance. Physically, at large z_a, the adatom should instead be considered as an isolated system. This failure of the LDA at large enough atom-surface distances is much more evident for adatom-induced resistivities than for charge contours or total energies, since it involves the DOS exactly at ϵ_F rather than its integral up to the Fermi level.

In order to obtain a physical, i.e., exponentially decaying ρ_s at large z_a, we propose an extrapolation scheme based on the effective-medium (EM) approach.[31] Far from the surface, we replace the z-dependent surface charge density with a simpler uniform charge density $\bar{n}_e$ obtained by averaging the surface charge density in a sphere of radius 3 a.u. around the adatom. We rewrite the resistivity in Eq. (5) as

$$\left(\frac{n_e}{\bar{n}_e}\right)^2 \rho_s = \frac{2\hbar}{V\pi \bar{n}_e^2 e^2} \int d\mathbf{r}\, d\mathbf{r}'\, \mathrm{Im}\, G(\mathbf{r},\mathbf{r}',\epsilon_F) \frac{\partial V_{\mathrm{eff}}}{\partial x'} \times \mathrm{Im}\, G(\mathbf{r}',\mathbf{r},\epsilon_F) \frac{\partial V_{\mathrm{eff}}}{\partial x}. \quad (13)$$

Since the right-hand side of Eq. (13) contains only information on the local electronic structure in the vicinity of the adatom, it may be approximated as $\rho_b(\bar{n}_e) = (4\pi\hbar/V\bar{n}_e e^2 \bar{k}_F) 5 \sin^2(\pi\tilde{Z}/10)$ in the spirit of the effective-medium approach, with $\tilde{Z}$ given by the calculated filling of the d orbital. Thus, for an adatom far enough from the metal, its induced resistivity is essentially given by the following effective medium expression ρ_s^{EM}, namely,

$$\rho_s^{EM} = \rho_b(\bar{n}_e) \frac{\bar{n}_e^2}{n_e^2}. \quad (14)$$

At very large z_a, ρ_s^{EM} decays as $\bar{n}_e^{2/3}$. In Fig. 4 we show the surface resistivity calculated with Eq. (14) by dot-dashed lines. Its values are of little significance in cases such as an adatom close to the jellium edge, where there is a strong inhomogeneity of the Fermi gas. But far from this, where the jellium electronic charge tail is slowly varying, they could provide an estimate of ρ_s. So the physically meaningful adatom induced resistivity is represented in Fig. 4 by the solid line, determined by the LDA-DFT calculation up to $z_a = 2$ a.u., and then by the effective-medium result at larger atom-metal distances.

Finally we remark that, to our knowledge, there has been no experimental work on the resistivity of $3d$ impurities on metal surfaces, although thin atomic layers of the $3d$ species were extensively studied in the past both theoretically and experimentally because of their importance for technological applications.[18,20,32,33] We observe from our results that the resistivity induced by a single adatom in the middle of a $3d$ series is much larger than that observed for Cu adatoms on Cu (0.6 ± 0.2 $\mu\Omega$ cm/at. %),[9] and for Au adatoms on Au (1.1 ± 0.1 $\mu\Omega$ cm/at. %).[34] Hence we expect that the resistivity change due to the $3d$ adatoms may easily be measured even at less than 0.1-ML coverages. By conducting an independent measurement for determining the coverage, for example, using scanning tunneling microscopy, it may be possible to estimate an absolute value of the surface resistivity induced by a single $3d$ adatom.

IV. CONCLUSIONS

In this paper we have presented an *ab initio* investigation of the surface-induced resistivity ρ_s of $3d$ nonmagnetic adatoms on a simple Al-like jellium surface. Differently from the same impurities in bulk, ρ_s is not only a function of the valence charge but of the atom-surface distance too. This property determines interesting features. In particular, we found that ρ_s, for an adatom very close to the jellium edge, may exceed that of the same bulk impurity. Such a result contrasts with intuition, since we are dealing with a system where the effective jellium density is indeed smaller. For Cr and Mn we examined the dependence of ρ_s on z_a in great detail, and located the position of the maximum of ρ_s, also discussing the physics leading to this. As a subject for future investigations, a theoretical calculation of the $3d$ adatoms within a spin-dependent LDA-DFT formalism could be important, because we foresee that such adatoms should display magnetic behavior, owing to the low density of the electronic jellium tail. We finally stress that our calculation refers to a single adatom. Though this model cannot deal with lateral effects which may affect the induced resistivity of $3d$ atom thin films, it can instead explore the elementary mechanism leading to resistivity, providing predictions for measurements performed at very low coverages. This is also the regime where electron-hole pairs effects,[31,35] closely related to the adatom-induced resistivity, are examined for atom-surface scattering and diffusion phenomena.

[1] J. Kondo, Prog. Theor. Phys. **32**, 37 (1964).
[2] J. Friedel, Nuovo Cimento, Suppl. **7**, 287 (1958).
[3] E. Babic, R. Krsnik, B. Leontic, M. Ocko, Z. Vucic, I. Zoric, and E. Girst, Solid State Commun. **10**, 691 (1972); G. Boato, M. Bugo, and C. Rizzuto, Nuovo Cimento **45**, 226 (1966).
[4] E. Mrosan and G. Lehmann, Phys. Status Solidi B **78**, 159 (1976).
[5] R.M. Nieminen and M. Puska, J. Phys. F: Met. Phys. **10**, L123 (1980).
[6] J. Deutz, P.H. Dederichs, and R. Zeller, J. Phys. F: Met. Phys. **11**, 1787 (1981).
[7] I. Mertig, E. Mrosan, R. Zeller, P.H. Dederichs, and P. Ziesche, Phys. Status Solidi B **117**, 335 (1983).
[8] I. Mertig, E. Mrosan, R. Zeller, and P.H. Dederichs, Phys. Status Solidi B **117**, 619 (1983).
[9] For a review, see D. Schumacher, *Surface Scattering Experiments with Conduction Electrons*, Springer Tracts in Modern Physics Vol. 128 (Springer, Berlin, 1993).
[10] K. Fuchs, Proc. Cambridge Philos. Soc. **34**, 100 (1938).
[11] E.H. Sondheimer, Adv. Phys. **1**, 1 (1952); M.S.P. Lucas, J. Appl. Phys. **36**, 1632 (1965).
[12] H. Ishida, Phys. Rev. B **52**, 10 819 (1995); **57**, 4140 (1998).
[13] H. Ishida, Phys. Rev. B **54**, 10 905 (1996).
[14] P.J. Rous, Phys. Rev. B **61**, 8484 (2000).
[15] P.J. Rous, J. Appl. Phys. **87**, 2780 (2000).
[16] N.D. Lang and W. Kohn, Phys. Rev. B **1**, 4555 (1970).
[17] J.E. Inglesfield, J. Phys. C **14**, 3795 (1981).
[18] W. Platov, U. Bovensiepen, P. Poulopoulos, M. Farle, K. Baberschke, L. Hammer, S. Walter, S. Müller, and K. Heinz, Phys. Rev. B **59**, 12 641 (1999).
[19] V.I. Gravilenko and R. Wu, Phys. Rev. B **60**, 9539 (1999).
[20] Z. Yang, V.I. Gravilenko, and R. Wu, Surf. Sci. **447**, 212 (2000).
[21] M.I. Trioni, G.P. Brivio, S. Crampin, and J.E. Inglesfield, Phys. Rev. B **53**, 8052 (1996).
[22] M.I. Trioni, S. Marcotulio, G. Santoro, V. Bortolani, G. Palumbo, and G.P. Brivio, Phys. Rev. B **58**, 11 043 (1998).
[23] N.D. Lang and A.R. Williams, Phys. Rev. B **18**, 616 (1978).
[24] W. Kohn and L.J. Sham, Phys. Rev. **140**, A1133 (1965).
[25] In the actual calculation, $R_{\mathrm{MT}}=2.8$ a.u., $R_s=7$ a.u., and $\tilde{a}=9.5$ a.u. The cutoff energy for the basis functions in the interstitial region is 16 Ry, and the maximum angular momentum for the Green-function expansion, $l_{\max}$, is chosen as 7.
[26] Note that 1.94 $\mu\Omega$ cm/at. %=1000 a.u. for Al.
[27] N. Bonini, M. I. Trioni, and G. P. Brivio, J. Chem. Phys. **113**, 5624 (2000).
[28] See Ref. 5 for the impurity resistivity of substitutional atoms in the bulk. In their calculation, the Al ion core at the origin is removed and replaced by a $3d$ nucleus to represent a $3d$ substitutional atom. The calculated ρ_b curve is similar to the interstitial result in Fig. 3, but is shifted toward the right mainly because of the different $3d$ occupation.
[29] B.N.J. Persson, Phys. Rev. B **44**, 3277 (1991).
[30] R. Podloucky, R. Zeller, and P.H. Dederichs, Phys. Rev. B **22**, 5777 (1990).
[31] G.P. Brivio and M.I. Trioni, Rev. Mod. Phys. **71**, 231 (1999).
[32] S. Handschuh and S. Blügel, Solid State Commun. **105**, 633 (1998).
[33] V.S. Stepanyuk, W. Hergert, P. Rennert, B. Nonas, R. Zeller, and P.H. Dederichs, Phys. Rev. B **61**, 2356 (2000).
[34] C. Pariset and J.P. Chauvineau, Surf. Sci. **78**, 478 (1978).
[35] G.P. Brivio and T.B. Grimley, Surf. Sci. Rep. **17**, 1 (1993).